Available online at www.sciencedirect.com

ScienceDirect

Ciência & Tecnologia dos Materiais 27 (2015) 84–91

Ciência & Tecnologia dos MATERIAIS

http://ees.elsevier.com/ctmat

Special Issue IJSI 2014

A study on the effect of weld induced residual stresses and the influence of weld sequencing of centrifugal extractor rotating bowl using numerical simulation and experimental validation

Satish K. Velaga*, G. Rajput, T. Selvaraj, B.M. Anandarao, A. Ravisankar

Reprocessing Plant Design Division, Reprocessing Group, Indira Gandhi Centre for Atomic Research, Department of Atomic Energy, Kalpakkam 603102, Tamil Nadu, India

Abstract

Centrifugal Extractors (CE) are the most preferred extraction equipment for the separation of fissile material from radioactive fission products in fast reactor spent fuel reprocessing in order to reduce damage to the solvent by minimizing the residence time. During fabrication of thin section high speed CE rotating bowls, several important factors such as heat input, weld speed, groove geometry, number of passes and weld sequencing are to be considered to control weld induced residual stresses and distortions. The thermal cycles due to concentrated heat input applied during the welding process, generates inhomogeneous plastic deformation and in turn the residual stresses in the weld metal. The presence of tensile residual stresses increase the susceptibility of a weld to fatigue damage, stress corrosion cracking (SCC) and fracture. A 3-D finite element analysis using SYSWELD software, for a three plane GTAW circumferential butt joint is carried out to predict weld induced residual stresses and distortions during fabrication of CE rotating bowls. The GTAW process was simulated using a nonlinear heat transfer analysis with the moving double ellipsoidal heat source model and a sequentially coupled thermo-metallo-mechanical analysis. This study includes temperature dependent thermo-physical, thermo-mechanical properties and isotropic hardening model. The axial and hoop residual stresses on the inner and outer surfaces are computed. Tensile residual stress on the inner surface and compressive residual stress on the outer surface are observed and their impacts on the CE rotating bowl are discussed. The importance of weld sequencing and its inference is investigated and validated against the experimental results.

Keywords: centrifugal extractors; weld sequencing; numerical simulation; weld distortion; residual stress.

1. Introduction

Centrifugal extractor banks are used in the fast reactor spent fuel reprocessing plants to recover valuable uranium and plutonium from radioactive solution leaving by solvent extraction step using 30% Tributyl phosphate in an alkane diluents as solvent [1]. The CE has the advantages of fine dispersion through shearing of liquid layers between the stationary and rotating bowls. In addition to this, it has fast phase separation due to high centrifugal field in the order of 200 to 1000g. This leads to reduced contact time and less radiation damage to solvent. Steady state is achieved faster and stage equilibrium will not be disturbed due to stoppage of unit unlike pulse columns or mixer settlers. A typical 16 stage CE bank assembly is shown in Figure 1.

* Corresponding author.
E-mail address: vsatish@igcar.gov.in, satish16@gmail.com (S.K. Velaga)

http://dx.doi.org/10.1016/j.ctmat.2015.03.011

Fig. 1. Sixteen stage centrifugal extractor bank assembly.

In the CE assembly the special features are (i) separation of individual phases in the rotating bowl due to centrifugal force and (ii) static head difference between mixer and the collection chamber which enables pumping to adjacent stage.

Ideally the CE rotating bowl, being a single integral unit that has to be machined as a single piece by special machining techniques. Since the above machining techniques are not available indigenously, rotating bowl components have to be machined individually then fitted, aligned and welded together. This type of thin section high speed rotating bowls are fabricated using electron beam welding where as we have adopted conventionally readily available pulse GTAW technique using special welding fixtures in order to control weld induced residual stresses and distortions. The material of construction is solution annealed austenitic stainless steel (SS) grade 304L with supplementary requirements such as Inter Granular Corrosion test as per ASTM A262 practice C. During fabrication of SS components it is important to note that SS has higher coefficients of thermal expansion and lower coefficients of thermal conductivity than carbon steels. This causes a greater tendency to weld distortion. The thermal cycles due to welding process produce inhomogeneous plastic deformation and residual stresses in the weld metal. The presence of tensile residual stresses increases the susceptibility of a weld to fatigue damage, SCC and fracture [2]. Further, the welding distortion has negative effects on the accuracy of assembly, geometrical tolerances and unbalance mass [3]. For these reasons, prediction and control of temperature distributions, residual stresses and welding distortions during and after the welding process is very important.

In the past decades, typical numerical analyses with supporting experimental data were established leading to ample fundamental knowledge about residual stress distributions [4-11]. Dean Deng et al. [11] employed both experiment and finite element method (FEM) to investigate the welding residual stress distribution in medium thick-walled austenitic stainless steel pipe. Besides, substantial amount of numerical simulation and experimental measurement, emphasizing on circumferential butt welding, is available in the literature [12-20]. Sattari-Far et al. [18] investigated the effect of welding sequence on welding deformations in circumferential butt welding of pipe to pipe joints of AISI 304 stainless steel. Chakrapani Basavaraju [19] developed an axisymmetric finite element evaluation of hoop shrinkage associated with circumferential butt welds in thin wall stainless steel pipes. Bachorski et al. [20] used linear elastic finite-element modelling technique to predict post-weld distortion in single-V butt welded plates.

However, very limited literature exists, describing the prediction of residual stresses and weld distortions in three plane circumferential butt welding of thin walled cylinders particularly for CE rotating bowls. Further a limited literature is available for the study of influence of weld sequencing on the weld induced residual stresses of CE rotating bowl by numerical simulation.

The objective of this work is to make a parametric study on the estimation of welding distortions for a typical GTAW welded three plane circumferential butt joint of CE rotating bowl. Further, the present work is undertaken to study distribution of residual stresses during and after the welding process of CE rotating bowl using FE simulation. Finite element method (FEM) is a well-established tool for accurate assessment of thermo-mechanical behaviour in circumferentially joined thin-walled structures and is being used in the evaluation of welding residual stress and distortions [4].

This paper presents a computational procedure for the evaluation of weld induced residual stresses and distortions for a typical GTAW welded three-plane circumferential butt joint of CE rotating bowl. Also, this paper presents a parametric study for the estimation of welding residual stresses and distortions. In this study, the total work executed is divided in to two parts. First part highlights the importance of weld sequencing by using the FE code weld planner in order to control distortions. Second part discusses the distribution of residual stresses in CE rotating bowl by carrying out thermo-metallurgical-mechanical analysis using SYSWELD.

2. Approach to the study

During the first part of this study, different cases of weld sequences are considered to study the variation in welding distortions based on numerical simulations. Three cylindrical components with an external

diameter of 42 mm, wall thickness of 2 mm and total length of 130 mm are considered for the simulation. A full 3-D model is used in the weld planner and their meshes with boundary conditions are shown in Figures 2(a) and 2(b) respectively.

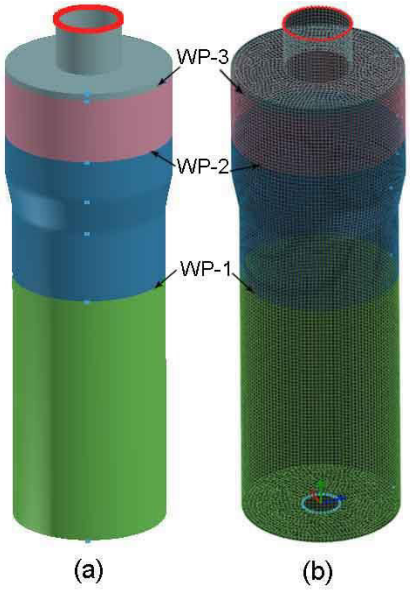

Fig. 2. (a) 3-D model and (b) FE mesh.

The analysis is performed using the FE code weld planner in SYSWELD [21]. The effects of tack welds on distortions are neglected in the analysis.

Initially, three dimensional heat conduction analysis was performed in order to obtain the temperature distribution history at all the nodes of the weld model. Further, the same thermal loads are employed in the subsequent thermo-metallurgical-mechanical analysis for the evaluation of weld distortions and residual stresses. The temperature-dependent thermo-physical properties such as density, thermal conductivity and specific heat and temperature-dependent thermo-mechanical properties such as coefficient of thermal expansion, Young's modulus and yield stress and are used for thermal and mechanical analyses respectively. The chemical composition, temperature dependent thermo-mechanical and thermo-physical properties of austenitic stainless steel (i.e. AISI 304L) that are used for numerical simulation are taken from Kim et al. [22] and Zhu et al. [23]. The isotropic hardening model with linear strain hardening behaviour is assumed for the analysis. FEM analysis is performed using SYSWELD software, applying same material properties for both the base and weld metal. The ambient temperature is assumed to be 25 ºC.

3. Finite element modelling

In order to make the accurate measurement of temperature distributions and residual stresses, FE mesh is developed in SYSWELD for the simulation of three plane butt joint of GTAW process. The 3-D FE mesh which is used for residual stress analysis is shown in Figure 3. The element type used is Quard-3-D solid with three translational degree of freedom at each node.

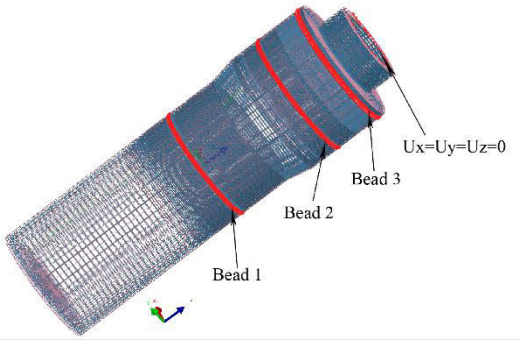

Fig. 3. FE mesh with boundary conditions.

3.1. Thermal model

The residual stresses are generally depended on non-uniform temperature distributions, generated during welding and are highly sensitive to transient temperature distributions. For the evaluation of realistic temperature history, thermal analysis is very important with appropriate boundary conditions such as heat transfer by conduction, heat losses due to thermal coefficient by convection and radiation and heat input from the weld source. In this study, the heat from the moving weld source is applied as a volumetric heat source with a double ellipsoidal distribution proposed by Goldak [24]. Thereafter, the temperature distribution within the component is modelled by the equation of conservation of energy, which tells that addition of volumetric heat conduction and heat generation rate are equal to thermal inertia.

3.2. Mechanical model

The stress analysis is carried out to evaluate state of stress induced during welding with complex boundary conditions. The same finite element model used in the thermal analysis is employed here, except for the boundary conditions. The boundary conditions used for mechanical analysis in order to prevent the rigid body motion are shown in Figure 3. The stress analysis is conducted using the temperature histories which are computed by the thermal analysis. In the evaluation of

the residual stresses due to the incompatible strains caused by thermal gradients and micro-structural changes, thermo-elasto-plastic formulations are required. Therefore, the total strain can be considered as the sum of the individual components such as elastic, plastic and thermo-metallurgical strain. However, for the considered material (AISI 304L), phase transformation has an insignificant effect. Hence, the strain due to phase transformation is not considered during the analysis.

4. Simulation results and discussion

This section deals with the results of effect of weld sequencing and the distributions of residual stresses in a three plane circumferentially butt welded CE rotating bowl.

4.1. Influence of weld sequencing

Five different cases are analysed for the welding sequence of CE rotating bowl, as shown in Figure 4.

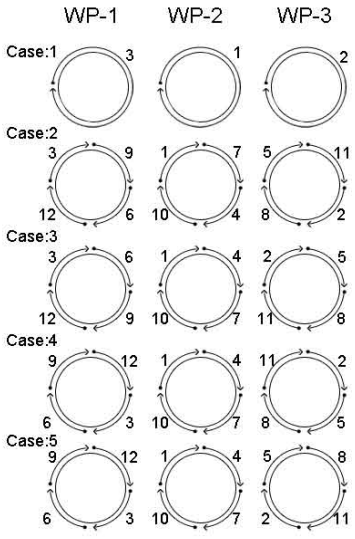

Fig. 4. Five different cases of weld sequencing.

In the case 1, weld is conducted entirely in each plane as one segment from the weld start location to the end location. For the remaining four cases, each weld plane is divided into 4 segments and the total of 12 segments is considered for this investigation as shown in Figure 4. Figure 5 shows the diameter variation/ distortion distribution and also compares the total distortion for five different cases of weld sequencing analysed by the numerical simulation.

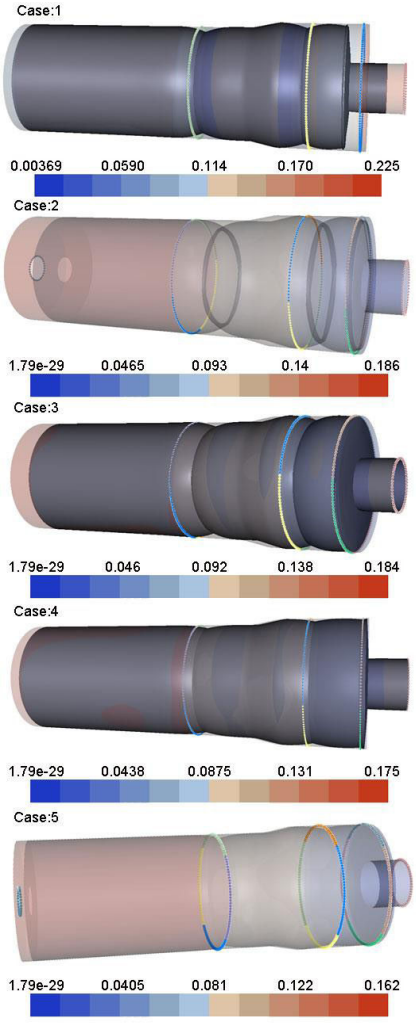

Fig. 5. Distortion contour plots of CE rotating bowl.

The diameter variation gives a value of the ovality of the component due to welding. This indicates that, the diameter of the component in the weld metal region and its vicinity reduces after welding. This bending deformation in the component generates stresses through the component thickness. The observations and the trends seen on the weld induced distortions in this study are found to be in agreement with the results reported in the literature [18]. Results of case-1 reveal that continuous welding in each plane gives higher radial distortion than the weld sequencing by four segments for each plane. It can be seen that there is considerable variation in distortions within the heat affected zone (HAZ) for the different cases as shown in Figure 5. For the cases 2 to 5, total of twelve segments are considered and with different weld sequencing weld distortion ranges from 186 microns to

162 microns are observed. Figure 5 reveals that welding according to cases 2 to 5 are good consequence to minimize welding distortion. This finding tells that increasing number of sequences in the circumferential welding process always leads to decrease in weld distortions.

4.2. Welding residual stress distribution on CE rotating bowl

During the analysis, three circumferential butt weld joints are considered to develop a CE rotating bowl and it is necessary to provide the weld joint totally from outside. These three butt weld joints are represented as bead 1, bead 2 and bead 3. It is proposed to divide each bead in to three segments, spacing 120º each. The FE model was run for one pattern of weld sequencing. The beads, segments and weld sequencing are shown in Figure 6.

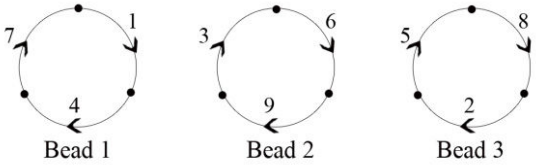

Fig. 6. Sequence of welding for all three beads.

To ascertain the influence of weld sequencing on the distribution of residual stresses thermo-metallurgical-mechanical analysis is performed and the parameters which are used during FE simulation are given in Table 1. The weld speed is considered as 0.5 mm/s and the simulation was run for a time period of 10,000 s.

Table 1. FE simulation parameters.

Case	Current (I) [amps]	Voltage [V] volts	Weld power= V×I [W]	Weld speed [mm/s]	Heat input [J/mm]
1	45-50	14	630-700	0.5	1260-1400

In case of butt weld joints of cylindrical components, stress normal to the direction of the weld bead is the axial residual stress, stress parallel to the direction of weld bead is the hoop residual stress and stress that acts towards or away from the central axis of a curved member is called the radial stress. The hoop residual stresses are generated due to expansion and contraction in radial direction during thermal cycling in the welding process. Variable shrinkage patterns through the wall thickness occur due to different temperature gradients generates radial residual stresses on both sides of WL. The contour plot of Von Mises stress distribution at 500 s is shown in Figure 7 and its maximum value is 298.3 MPa.

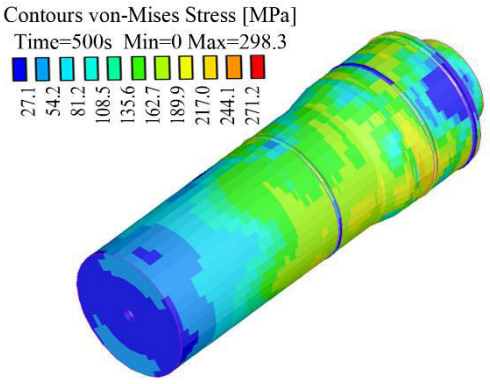

Fig.7. Contours of von Mises stress.

The weld process takes about 1100 s to complete all the three plane circumferential butt welds. In the mechanical analysis axial, hoop and radial residual stresses were simulated on inner and outer surfaces for cases immediately after completion of weld (i.e., at 1100 s) and after cooling the work piece to 10000 s. Figures 8 and 9 show the axial, hoop and radial residual stress distributions on the inner surface after completion of weld (i.e., at 1100 s) and after cooling the work piece to 10000 s respectively.

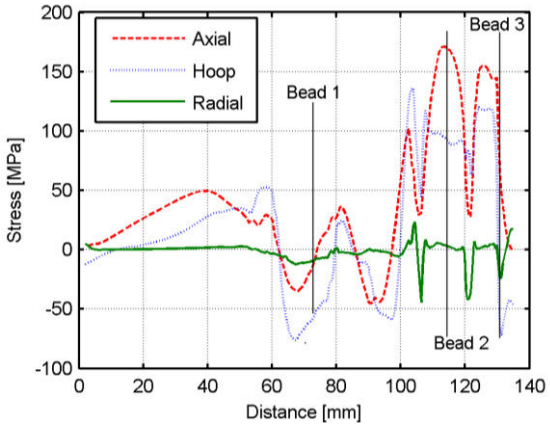

Fig. 8. Stress distribution at t=1100 s on the inner surface.

Figures 10 and 11 depict stress distributions on the outer surface at 1100 s and at 10000 s respectively. Stress distributions on the inner and outer surfaces were taken at 180º cross-section from the weld start position.

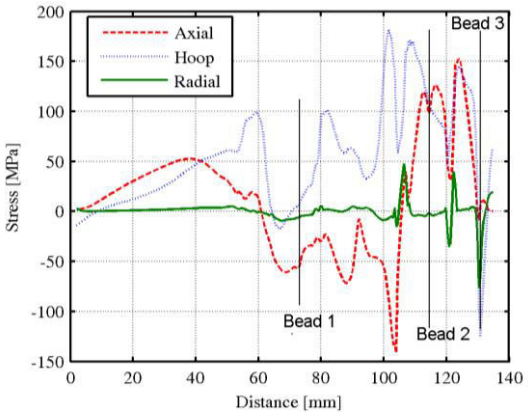

Fig. 9. Stress distribution at t=10,000 s on the inner surface.

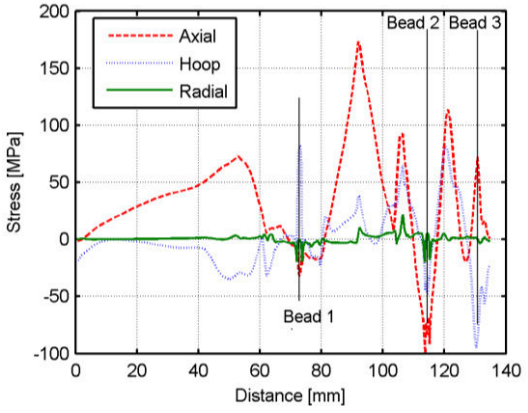

Fig. 10. Stress distribution at t=1100 s on the outer surface.

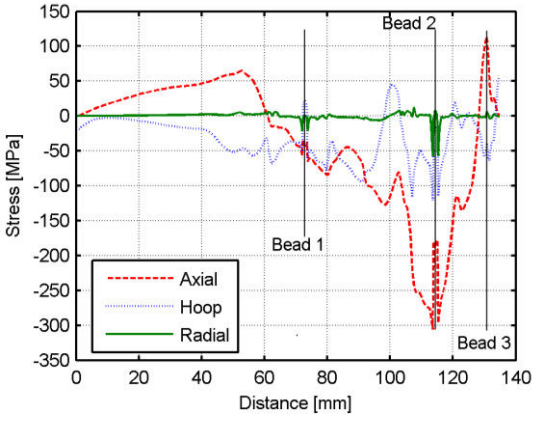

Fig. 11. Stress distribution at t=10,000 s on the outer surface.

From these figures, it can be seen that the stresses are both tensile and compressive due to temperature gradients, uneven shrinkage and the type of boundary conditions. On the inner surface, at bead 1, compressive axial stress field is noticed near the high temperature region. Whereas, a tensile stress is formed in the low temperature region. The reason for this could be, as the time progresses the temperature in the weld zone decreases; whereas in the surrounding region, temperatures start to increase due to law of conduction from weld bead. This causes the weld metal close to bead to contract, and away from bead to expand. Figures 8 and 9 illustrate that at bead 1, compressive hoop stresses are predicted at the heat affected zone at t = 1100 s, while tensile hoop stresses (comparatively) emerge in the newly solidified metal at t = 10000 s for hoop stress. In general, the trend for the axial and hoop stresses at the weld zone on the inner surface is tensile which are in line with the results published in [3,4]. In this study, tensile hoop and axial stresses are observed at bead 2 and these are in the range of 100 to 150 MPa. Bead 3 is very close to the top plate and nearer to the boundary condition as shown in Figure 3. Hence, at bead 3 compressive axial and hoop stresses are generated which are negligible and localized.

On the other hand, the results of axial and hoop stresses on the outer surface show an opposite trend at bead 2. Figures 8-11, also exhibit the radial stress distribution on the inner and outer surfaces at times t = 1100 s and t = 10000 s. An interesting observation to note is that unlike the hoop and axial stresses, the radial stresses are not influenced by time. It can also be seen that the radial stresses are negligible on both sides of the weld location on the inner and outer surface. At bead 2, the transition of axial and hoop stresses from compressive to tensile is obtained near the heat affected zone at t = 1100 s, whereas the transition from compressive to tensile is observed away from the heat affected zone at t = 10000 s as shown in Figures 10 and 11. The trends for axial and hoop stresses at bead 2 also concur well with the observations recorded by the previous researchers [3-5,11]. The magnitude of hoop and axial stresses at bead 1 on the inner and outer surfaces are very less and that may be attributed to reasons such as no constraints at the bottom side of the CE rotating bowl and weld sequencing for all three circumferential butt joints.

5. Experimental validation

To ensure the reliability and for comparison with numerical simulation results, GTAW experiments are conducted and is shown in Figure 12(a). The experiments are performed for one pattern of weld sequencing as shown in Figure 6. The three cylinders and an end plate are initially joined by four tack welds (each 90º apart) at each bead. Experimental residual stress measurement using X-ray diffraction method is an established technique. In this technique, strain in the surface layers of a material is estimated by measuring

the shift in the position of the diffraction peak of a set of parallel planes. These strains are then converted into stresses analytically using various assumptions.

Axial residual stresses are measured at the weld centres of bead 1 and 2 at the 180º plane and 300º plane respectively. Similarly, hoop stresses are also measured at the same locations. The quantitative comparison of measured values and simulated nodal residual stresses at the weld centre is shown in Figure 12(b). It is evident that simulated results are in a good agreement with the experimental data, thus the numerical simulations are experimentally validated.

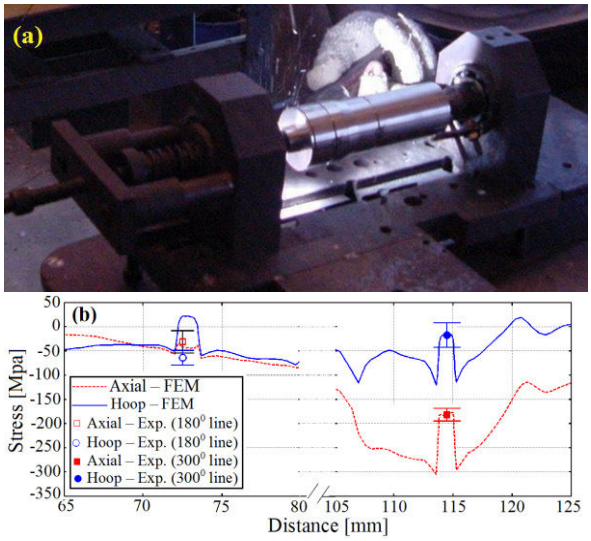

Fig. 12. (a) Experimental setup and (b) experimental validation of residual stresses.

6. Conclusions

This study performs a finite element analysis of the residual stress and weld distortions in the AISI 304 L stainless steel CE rotating bowl with different weld sequences in a three plane circumferentially butt welded joint. The following conclusions are drawn:

(1) Radial weld distortions from 3-D numerical analysis are predicted.
(2) The weld distortion in the HAZ area with one segment in each plane could be decreased by using a sequence of four segments in each plane, indicating the benefits of welding sequence to decrease the welding distortions.
(3) The maximum tensile axial and hoop stresses are generated at the weld bead 2 on the inner surface. Whereas, the peak compressive axial stress is noticed at bead 2 on the outer surface.
(4) The results of the FE simulation revealed that the radial residual stresses are found to be negligible. Magnitudes of axial and hoop residual stresses are found to be lesser in this study when compared to single plane continuous circumferential butt weld joint. The residual stress induced is below the yield strength of the material in this study. This reduces the susceptibility of the weld to fatigue damage, stress corrosion cracking and fracture.
(5) The numerical results for residual stress distributions obtained were in good agreement with those obtained by the X-ray experiments.

Acknowledgments

The authors would like to thank Dr. B.P.C Rao and Mr. S. Mahadevan, IGCAR for help with metallurgical examinations and Dr. S. Venugopal, IGCAR for useful discussions and suggestions. We also sincerely thank Dr. R. Natarajan, Director, Reprocessing Group and Dr. P.R. Vasudeva Rao, Director, IGCAR for their constant encouragement and support.

References

[1] G.J. Bernstein, D.E. Grosvenor, J.F. Lenc, N.M Levitz, ANL - 7968, USA, 1973.
[2] S. Murugan, S.K. Rai, P.V. Kumar, T. Jayakumar, Baldev Raj, M.S.C. Bose, Int. J. Pressure Vessels Piping. 78 (2001) 307–317.
[3] A. Ravisankar, S.K. Velaga, G. Rajput, S. Murugan, S. Venugopal, Int. conference on advances in manufacturing technology – ICAMT, Chennai, 2012.
[4] A.M. Malik, E.M. Qureshi, N.U. Dar, I. Khan, Thin Wall. Struct. 46 (2008) 1391-1401.
[5] D. Deng, H. Murakawa, Comp. Mater. Sci. 37 (2006) 269-277.
[6] C.-H. Lee, K.-H. Chang, Mater. Sci. Eng: A. 487 (2008) 210-218.
[7] T.-L. Teng, C.-P. Fung, P.-H. Chang, W.C. Yang, Int. J. Pressure Vessels Piping. 78 (2001) 523-538.
[8] Y. Shim, F. Feng, S. Lee, D. Kim, J. Jaeger, J.C. Papritan, C.L. Tsai, Welding J. 71 (1992) 305s–312s.
[9] P.-H. Chang, T.-L. Teng, Comp. Mater. Sci. 29 (2004) 511-522.
[10] S. Kiyoshima, D. Deng, K. Ogawa, N. Yanagida Saito, Comp. Mater. Sci. 46 (2009) 987-995.
[11] D. Deng, H. Murakawa, W. Liang, Comp. Mater. Sci. 42 (2008) 234-244.
[12] B. Brickstad, B.L. Josefson, Int. J. Pressure Vessels Piping 75 (1998) 11-25.

[13] E.F. Rybicki, D.W. Schmueser, R.W. Stonesifer, J.J. Groom, H.W. Mishaler, J. Pressure Vessel Technol. 100 (1978) 256-262.
14] L. Karlsson, M. Jonsson, L.E. Lindgren, M. Nasstrom, L. Troive, ASME pressure vessels and piping conference, 173, Hawai: Honolulu, 1989.
[15] Y. Dong, J. Hong, C. Tasi, P. Dong, AWS Weld J. 442 (1997) 444-449.
[16] R.I. Karlsson, B.L. Josefson, J. Press. Vessel Technol. 112 (1990) 76-84.
[17] S. Fricke, E. Keim, J. Schmidt, Nucl. Eng. Des. 206 (2001) 139-150.
[18] I. Sattari-Far, Y. Javadi, Int. J. Pressure Vessels Piping 85 (2008) 265-274.
[19] C. Basavaraju, Nucl. Eng. Des. 197 (2000) 239-247.
[20] A. Bachorski, M.J. Painter, A.J. Smailes, M.A. Wahab, J. Mater. Proc. Tech. 92 (1999) 405-409.
[21] Sysweld reference manual and material data, ESI group, 2005.
[22] Y.C. Kim, A. Fuji, T.H. North, Mater. Sci. Technol. 11 (1995) 383-388.
[23] X.K. Zhu, Y.J. Chao, J. Mater. Proc. Tech. 146 (2004) 263-272.
[24] J. Goldak, A. Chakravarti, M. Bibby, Metall. Trans. B. 15B (1984) 299-305.